N72-21952

NASA TECHNICAL MEMORANDUM

NASA TM X-68044

NASA TM X-68044

CASE FILE COPY

OPTICAL PROPERTIES OF THERMAL CONTROL COATINGS CONTAMINATED BY MMH/N_2O_4 5-POUND THRUSTER IN A VACUUM ENVIRONMENT WITH SOLAR SIMULATION

by R. D. Sommers, C. A. Raquet, and J. F. Cassidy
Lewis Research Center
Cleveland, Ohio

TECHNICAL PAPER proposed for presentation at
Seventh Thermophysics Conference sponsored by the
American Institute of Aeronautics and Astronautics
San Antonio, Texas, April 10-12, 1972

OPTICAL PROPERTIES OF THERMAL CONTROL COATINGS CONTAMINATED BY MMH/N_2O_4 5-POUND THRUSTER IN A VACUUM ENVIRONMENT WITH SOLAR SIMULATION

by R. D. Sommers, C. A. Raquet, and J. F. Cassidy

Lewis Research Center
National Aeronautics and Space Administration
Cleveland, Ohio

E-6881

Abstract

Cat-a-lac Black, and S13G thermal control coatings were exposed to the exhaust of a thruster in a simulated space environment. Vacuum was maintained at less than 10^{-5} torr during thruster firing in the liquid helium cooled facility. The thruster was fired in a 50-millisecond pulse mode and the accumulated firing time was 224 seconds. Solar absorptance (α_s) and thermal emittance (ϵ) of the coatings were measured in-situ at intervals of 300 pulses. A calorimetric technique was used to measure α_s and ϵ. The tests, technique, and test results are presented.

The Cat-a-lac Black coatings showed no change in α_s or ϵ. The S13G showed up to 25 percent increase in α_s but no change in ϵ.

Introduction

Many spacecraft surfaces are exposed to the exhaust plumes of propulsion and attitude control thrusters. Some of these surfaces are commonly used as passive thermal control surfaces and are treated (by painting, polishing, etc.) so as to have particular optical properties (emittance, solar absorptance). The exhaust plume - spacecraft surface interaction may be such that changes in the optical properties of the surface occur. If such changes occur, then the thermal balance of the spacecraft may be altered, resulting in intolerable spacecraft temperatures.

To study properly exhaust plume effects on thermal control coatings on spacecraft, a thruster must be fired in a high vacuum environment which must be maintained during the firing. Changes of the coatings should be measured while the coatings remain in the environment. Two main reasons dictate these requirements: (1) presence of an atmosphere would cause the exhaust plume to be different from plumes in space, altering the manner in which the plume impinges on nearby surfaces, and (2) removal of the coatings for optical measurements would expose them to atmospheric effects and perhaps alter the observable damage.

Previous plume damage studies in the literature[1-7] indicated the degree to which optical coatings are damaged by rocket exhaust plumes and showed a wide range of degradation effects. But in most instances in-situ measurements were not made, or coatings were exposed to the atmosphere during the rocket firings.

This paper reports the rocket plume contamination effects on two types of thermal control coatings - white S13G and Cat-a-lac black. Measurements of α_s and ϵ were made in a space simulation chamber providing a vacuum environment of less than 10^{-5} torr, liquid helium or 20° K gaseous helium cooled surroundings, and solar radiation simulated by a carbon arc lamp with a good solar spectral match. The in-situ measurements of α_s and ϵ followed firings of an MMH/N_2O_4 5-lb thrust scaled down version of the Marquardt R4D 22-lb thrust RCS thruster.

Experiment

The rocket firings and optical measurements were made in the Lewis Research Center's 6 × 12-foot liquid helium cooled space simulator described in Ref. 8. A schematic of the space chamber and thruster installation is shown in Fig. 1.

The thruster being used is a 5-lb thrust version of the MOL reaction control system thruster (Marquardt Co.). The engine propellant system consisted of monomethylhydrazine (MMH) and nitrogen tetroxide (N_2O_4). Both propellants were maintained between 13° C to 20° C. The injector is a single doublet and the thruster is radiation cooled. Table I lists the primary design and performance features of the thruster.

Early cryopumping studies in the Lewis Research Center's liquid helium-cooled facility showed two significant advantages of this facility over the conventionally pumped space chambers. First, large amounts of room temperature hydrogen (3 liters/sec at standard conditions) could be cryopumped at a pressure of 3×10^{-5} torr. Second, the amount of hydrogen that could be cryopumped was increased by the addition of condensable gases.[8] Since the exhaust products of a bipropellant engine using MMH/N_2O_4 contains hydrogen as well as condensable gases such as H_2O, CO_2, CO, and N_2, it was expected that these condensable gases would provide additional cryopumping of the hot hydrogen gas. Rocket plume pumping tests performed in this facility show that starting with an initial pressure of 2×10^{-9} torr, a 50-millisecond firing of the 5-lb thrust, bipropellant thruster increases the ambient pressure only to 2×10^{-5} torr. Subsequently, the pressure was cryopumped very quickly back to the 2×10^{-9} torr level within 100 milliseconds. These results established that good space simulation could be achieved if the minimum time between firing pulses was 100 milliseconds.

Ambient pressure instrumentation within the cryopumped facility consists of a buried collector hot-ionization gauge with an electrometer connected directly to the collector. The total response time of the electrometer and the buried collector gauge is 100 microseconds per decade. Figure 2 is an oscilloscope trace of the buried collector gauge, indicating the changes in test section pressure during a pulse train. Trace "A" records the power applied to the valves and is used as a marker trace. The pre-firing test section pressure is 7×10^{-7} mm Hg and on firing the thruster the test section pressure increases to 3×10^{-5} mm Hg for all pulses. The test section pressure decreases to

1×10^{-5} mm Hg after the first four pulses but continues at the firing pressure after the remaining pulses. The test section pressure decreases to its initial value of 7×10^{-7} mm Hg in 7 minutes. This time also allows the thruster temperatures to return to initial conditions. Subsequently, the engine is fired for another set of eight pulses. Figure 2 indicates that space simulation pressures corresponding to altitudes of 130 km or greater were maintained during the engine firing schedule followed using cryopumping test section walls at liquid helium temperature.

Solar radiation is provided by a 28 kW carbon arc lamp which projects a collimated beam of radiation into the chamber.(9) The beam intensity can be controlled over the range of 0.5 to 1.0 solar constants (700 - 1400 W/m^2) and is measured by radiometers installed in the plane of the samples. The radiometers are protected from plume contamination by electrically actuated covers which can be opened and closed remotely. The covers are open during the optical measurements and closed during rocket firings.

Rocket firing was done over a period of several weeks during which a day of rocket firing alternated with a day, or weekend, of standby for liquid helium reclamation. During standby conditions the space chamber was held at vacuum but allowed to warm up to room temperature.

A day of rocket operation consisted of about 6 hours during which the rocket was fired at intervals of 7 minutes. Each firing was a train of 8 pulses of 50 millisecond duration with 100 milliseconds between pulses. On the first day of the experiment two 200-millisecond checkout pulses were fired and several pulse trains of less than eight 50-millisecond pulses preceeded the regular schedule of trains of light 50-millisecond pulses.

Thermal measurements (heating of samples by solar radiation and then cooling) were made in the mornings and evenings of rocket firing days. As the experiment progressed and deposits collected on test surfaces, a question of possible evaporation of exhaust products from the samples during thermal measurements arose. In order to investigate such a possibility, a longer period of rocket operation was scheduled between thermal measurements near the end of the experiment.

In all, a total thruster firing time of 224 seconds (4476 pulses) was achieved over the course of the experiment.

Test Samples

The test samples are stainless steel type 302 discs 0.0127 cm thick and 2.46 cm in diameter. S13G and Cat-a-lac black paint coatings were put on the stainless steel substrates at Marshall Space Flight Center in accordance with George C. Marshall Space Flight Center Specifications.*

The substrates were weighed before and after the paints were applied. Initial values of α_s and ϵ were also measured at Marshall Space Flight Center after the painting. Table II lists properties of the test samples. Specific heat values for these coating materials and the stainless steel substrates were taken from Ref. 10.

Test samples are mounted in individual aluminum cups on three thin plastic pegs (Figs. 3 and 4). Copper-constantan thermocouples are spot welded to the back center of the test sample and to the inside of the cup. The thermocouples are terminated at a plug at the bottom of the cup.

Test samples and mounting cups are secured in a pallet mounted parallel to and $10\frac{1}{2}$ cm below the thruster nozzle axis. Locations of the samples in the pallet are shown in Fig. 5.

The pallet consists of a 0.625 cm thick aluminum sample holder plate and a thin radiative heater clamped to the holder plate. In the experiment the pallet is painted black and maintained at temperatures in the range 230° to 260° K. The pallet assembly with unpainted samples is shown in Fig. 6.

Data Reduction and Analysis

Thermal/optical measurements are made by heating the sample with the solar beam, allowing them to cool and then calculating solar absorptance and thermal emittance from the heating and cooling rates. Similar measurement techniques have been previously used and discussed by others and ourselves.(11,12)

The present experiment includes the use of automatic high-speed data recording and a time-shared computer. This allows the data to be recorded and managed more easily and permits the use of a more complex and complete thermal model.

The thermal model used includes solar heating, sample-mounting cup heat exchange, sample radiation, and engine-shroud heating. Equation (1) expresses the basic thermal model.

$$A\rho c_p d \frac{dT_s}{dt} = -\epsilon\sigma A T_s^4 - K_r\left(T_s^4 - T_m^4\right) + \alpha_s \varphi A + S T_{shrd}^4 \qquad (1)$$

where

A test surface area

ρ density

c_p specific heat

d thickness

T_s coating temperature

*Cat-a-lac Black - Carbon black pigment in epoxy resin with amine curing system. Proprietary formulation of Finch Paint and Chemical Company Application per Specification 10M01832. Cured: 16 hours at room temperature, 24 hours at 200° F in air circulating oven; thickness factor, 40 in.^{2}-mil/gm. S13G - Potassium silicate treated zinc oxide in dimethylsiloxane; Formulation per Specification 10M01835; Application per Specification 10M01836; Cured 40 hours at room temperature, 24 hours at 200° F in air circulating oven; Thickness factor, 32 in.^{2}-mil/gm.

T_m mounting cup temperature

T_{shrd} thruster package (shroud) temperature

t time

ϵ thermal emittance

σ Stefan Boltzmann constant

K_r radiation transfer coefficient between mounting cup and test surface

α_s solar absorptance

φ solar radiation flux

S radiation transfer coefficient between test surface and thruster package (shroud)

Analysis of the data proceeds as is schematically shown in Fig. 7. A computer curve fit is done to fit sample temperature as a function of time. From this fit, the derivative dT_s/dt is calculated. Equation (1) is then rearranged as

$$\left[\frac{\rho c_p d}{T_m^4}\frac{dT_s}{dt} - \frac{S}{A}\frac{T_{shrd}^4}{T_m^4}\right] = -\left(\sigma\epsilon + \frac{K_r}{A}\right)\left[\frac{T_s^4}{T_m^4}\right] + \frac{K_r}{A} \tag{2}$$

in the case of cooling, or in the form

$$\left[\frac{\rho c_p d}{\varphi}\frac{dT_s}{dt} - \frac{ST_{shrd}^4}{A\varphi} - \frac{K_r}{A}\frac{T_m^4}{\varphi}\right] = -\left(\sigma\epsilon + \frac{K_r}{A}\right)\left[\frac{T_s^4}{\varphi}\right] + \alpha_s \tag{3}$$

in the case of heating.

By performing a linear fit in the form $[\,] = a[\,] + b$ of the quantities in brackets in the cooling Eq. (2), the values of K_r and are determined.

$$K_r = b_c A \tag{4}$$

$$\epsilon = -\left(\frac{a_c}{\sigma} + \frac{K_r}{\sigma A}\right) \tag{5}$$

where the subscript 'c' refers to cooling. Having determined K_r, the process can be repeated with the heating Eq. (3) yielding

$$\alpha_s = b_h \tag{6}$$

$$\epsilon = -\left(\frac{a_h}{\sigma} + \frac{K_r}{\sigma A}\right) \tag{7}$$

and the subscript 'h' refers to heating.

A specialization is possible when the sample temperature intersects the mounting temperature. At that intersection sample-cup heat exchange term vanishes and ϵ and α_s are calculated from the cooling and heating data respectively as

$$\epsilon_i = \frac{\frac{S}{A}T_{shrd}^4 - \rho c_p d\frac{dT_s}{dt}}{\sigma T_s^4} \tag{8}$$

$$\alpha_{s_i} = \frac{\rho c_p d}{\varphi}\frac{dT_s}{dt} + \frac{\epsilon_i\sigma}{\varphi}T_s^4 - \frac{S}{A\varphi}T_{shrd}^4 \tag{9}$$

where the subscript i refers to values determined at the sample and cup temperature intersections.

The quantity S in the above equations represents the sample heating by the rocket shroud which nominally is held at 300° K. The value of S for each sample was determined in prefiring tests using known values of ϵ and α_s of the samples.[10] S was assumed to be constant throughout the rocket firing tests. The term containing S in Eq. (1) is significant only during cooling but it is included in the analysis of the heating data also.

Test Results

Test data for the coatings are shown in Figs. 8 and 9. The optical data shown were calculated by the cup-sample temperature intersection technique discussion earlier. The data was also analyzed by the curve fitting technique. It must be noted, however, that this technique assumes the temperature independence of K_r, ϵ, and α over the rather large temperature interval over which the measurements were made. Because the intersection technique eliminates K_r from consideration and calculates ϵ and α over a small temperature range (230°-250° K), effects of any temperature dependence of these quantities are reduced. The results obtained from the curve fitting technique are consistent with those of the intersection technique.

The white S13G coatings are located below the thruster axis (fig. 5) and show position dependent effects. Sample 29, closest to the thruster, shows less increase ($\Delta s_i = 0.03$) in α_{s_i} than does sample 28 ($\Delta\alpha_{s_i} = 0.05$) which is furthest from the thruster. This difference may be due to the closer sample not being fully immersed in the exhaust plume. Evidence that sample 29 is not as exposed to the plume as sample 28 is found in the plume heating of the samples. Table III lists typical temperature changes and heat gains during a pulse train (8 pulses, 50 milliseconds on, 100 milliseconds off). The close samples, both black and white, show approximately half the heat gain of the samples further away from the thruster. Visual inspection of the samples after the test bore out the position dependency of the damage. The close white sample (no. 29) was only slightly discolored. The middle sample (no. 27) had very many tiny reddish speckles on its surface. And the far sample (no. 28) had many larger reddish spots on it. These spots ranged up to a millimeter in size.

Thus the solar absorptance of S13G placed parallel to the rocket exhaust has increased 10 to 25 percent depending on position of the sample. The thermal emittance, ϵ_i, of the S13G samples seems to have been unaffected throughout the tests. The Cat-a-lac black samples show no long term changes in either α_{s_i} or ϵ_i.

During test measurements the α_{s_i} of the black and white coatings are affected by the method of obtaining the data. The thermal measure-

ments consist of several heating and cooling periods done sequentially. Each cooling yields a calculated ϵ_i, and each heating yields an α_{s_i}. We have noticed that the very first sample heating after a day's firing of thruster yields an extremely low α_{s_i} for the black samples, and a slightly low α_{s_i} for the white samples. The second and third heatings yield higher values than the first heating for α_{s_i} but are consistant with each other. The thermal emittance does not show any marked change during the several heating and cooling periods. Table IV compares a typical set of optical values with the change between first and second heatings after a long exposure to the rocket plume and before any exposure.

The data presented in Figs. 8 and 9 represent the α_{s_i} and ϵ_i values calculated from the last heating and cooling cycle of any given series of consecutive cycles (usually 3).

Condensation of plume exhaust products and their evaporation is one explanation for the initial lowering of α_{s_i} values. Condensate may be built up on the samples during thruster firing, and evaporated during the first heating period of the thermal measurements. If this is so, the condensate has the feature of a low α_{s_i} and a high thermal emittance. Based on the only slight lowering of the initial α_{s_i} for the S13G samples, the condensate (if there is one) may have an α_s of about 0.2. And based on the apparent lack of effect on the ϵ_i values the condensate may have a thermal emittance of about 0.8. Several gas condensates have these kinds of optical properties such as H_2O, N_2, CO, and CO_2 which are large fractions of the thruster exhaust.[1] Of these H_2O and CO_2 are the most likely condensate at the sample temperatures (200°-230° K).

Concluding Remarks

In-situ measurements of the optical properties of two types of thermal control coatings exposed to rocket exhaust plumes were made. Metal discs coated with white S13G and Cat-a-lac black coatings were placed parallel to the thruster axis and within its plume. The 5-lb thruster was fired on a pulsed mode in a liquid helium cooled space simulatione chamber. At the start of a pulse environment pressure was 5×10^{-7} mm Hg. During the engine pulsing, the chamber pressure always remained below 10^{-5} mm Hg. Thermal measurements were made of the solar absorptance α_s and thermal emittance ϵ of the coating during the several weeks of thruster firing without exposing the coatings to atmosphere.

After 224 seconds of thruster firing time the Cat-a-lac black coatings showed no permanent change in α_{s_i} or ϵ_i. The S13G coatings showed between 10 and 25 percent increase in α_{s_i} depending on where the coating was located. The thermal emittance of the S13G coating was unaffected.

There was evidence that some exhaust products condensed on the coatings during thruster firings and could have evaporated or changed chemically during exposure to a one solar constant radiation flux.

Acknowledgement

The paint coatings used in this study were prepared and applied by Marshall King, Materials Division, Marshall Space Flight Center.

References

1. Borson, E. N. and Landsbaum, E. M., "A Review of Available Rocket Contamination Results," TR-0200(4250-20)-2, SAMSO-TR-69-82, AD-850122L, Dec. 15, 1968, Aerospace Corp., El Segundo, Calif.
2. Burch, B. A., "Effect of Contamination on Spacecraft Surfaces Exposed to Rocket Exhaust," AEDC-TR-68-23, AD-831624L, Apr. 1968, ARO, Inc., Arnold Air Force Station, Tenn.
3. Yanizeski, G. M., "A Review of Thermal Control Coating Degradation by the Service Module Reaction Control System Rocket Exhaust and Estimated Effects on Skylab," TM-70-1022-12, NASA CR-113814, Sept. 21, 1970, Bellcomm, Inc., Washington, D.C.
4. Takimoto, H. H. and Denault, G. C., "Rocket Plume (N_2O_4/MMH) Impingement on an Aluminum Surface," TR-0066(5210-10)-7, SAMSO-TR-70-191, AD-707109, Mar. 15, 1970, Aerospace Corp., El Segundo, Calif.
5. Lyon, W. C., "Thruster Exhaust Effects upon Spacecraft," TM X-65427, 1970, NASA, Greenbelt, Md.
6. Arnett, G. M., "Lunar Excursion Module RCS Engine Vacuum Chamber Contamination Study," TM X-53859, 1969, NASA, Huntsville, Ala.
7. McCargo, M., Spradley, L. W., Greenberg, S. A., and McDonald, S. L., "Review of the Transient Degradation/Contamination of Thermal Control Coatings," LMSC-D177876, NASA CR-119898, May 1971, Lockheed Missiles and Space Co., Sunnyvale, Calif.
8. Cassidy, J. F., "Space Simulation Experiments on Reaction Control System Thruster Plumes," Proposed Technical Note, 1972, NASA, Cleveland, Ohio.
9. Uguccini, O. W. and Pollack, J. L., "A Carcon-Arc Solar Simulator," Paper 62-WA-241, Nov. 1962, ASME, New York, N.Y.
10. Spisz, E. W. and Jack, J. R., "Thermal and Radiative Property Measurement of Thermal Control Coatings by Cyclic Radiation," TN D-6316, 1971, NASA, Cleveland, Ohio.
11. Fussell, W. B., Triolo, J. J. and Henniger, J. H., "A Dynamic Thermal Vacuum Technique for Measuring the Solar Adsorption and Thermal Emittance of Spacecraft Coatings," <u>Measurement of Thermal Radiation Properties of Solids</u>, SP-31, 1963, NASA, Washington, D.C., pp. 83-101.
12. Mark, H., Sommers, R. D., and Mirtich, M. J., "Effect on Surface Thermal Properties of Calibrated Exposure to Micrometeoroid Environment," <u>AIAA Journal</u>, Vol. 4, No. 10, Oct. 1966, pp. 1811-1817.

E-6881

Table I Design and performance characteristics of 5-lb thruster

(a) Dribble volume oxidizer manifold = 0.00058 in.^{3}
(b) Dribble volume fuel manifold = 0.00113 in.^{3}
(c) Injector = single doublet
(d) Oxidizer injector orifice diameter = 0.0186 in.
(e) Fuel injector orifice diameter = 0.0158 in.
(f) L^* = 4.5
(g) Nozzle throat area = 0.0298 in.^{2}
(h) Nozzle area ratio = 39.2
(i) Nozzle contraction ratio = 4.2
(j) Oxidizer - fuel ratio = 1.6
(k) Fuel and oxidizer value opening time = 8 msec
(l) Fuel and oxidizer value closing time = 10 msec
(m) Ignition lag = 3 msec
(n) Thrust = 5-lb
(o) Specific impulse = 286 sec
(p) Total propellant flow rate = 0.0175 lb/sec
(q) Steady state nominal oxidizer flow = 0.011 lb/sec
(r) Steady state nominal fuel flow for, O/F ratio = 1.6, = 0.0065 lb/sec
(s) Combustion chamber pressure = 100 psi

Table 2 Coating properties[1]

Sample number and type	Initial* α_s	Initial* ϵ	Substrate weight, gm	Substrate plus coating, gm
No. 27 S13G	0.22	0.90	0.5825	0.7241
No. 28 S13G	.20	.90	.5822	.7470
No. 29 S13G	.20	.90	.5853	.7275
No. 7 Cat-a-lac Black	.95	.90	.5848	.6169
No. 8 Cat-a-lac Black	.95	.90	.5842	.6171

[1]Measured at George C. Marshall Space Flight Center.
*Measured on monitor samples prepared at the same time as the test coatings.

Table 3 Plume heating of samples

Horizontal distance from nozzle, cm	Type	T_i °K	T_f^1 °K	ΔT °K	Heat gain, cal/cm^2	$\Delta\alpha_{s_i}$
5.55	No. 29 S13G	215	219	4	0.059	0.03
9.62	No. 7 Cat-a-lac Black	216	223	7	.072	----
17.92	No. 27 S13G	206	215	9	.132	.04
30.32	No. 8 Cat-a-lac Black	203	214	11	.110	----
34.42	No. 28 S13G	200	208	8	.121	.05

[1]Measured within 9 seconds after thruster firing.

Table 4 Typical effect of heating on exposed samples

Heating cycle	Sample No. 27 S13G		Sample No. 8 cat-a-lac black	
	α_{s_i} Engine firing time = 0	α_{s_i} Engine firing time = 57 sec	α_{s_i} Engine firing time = 0	α_{s_i} Engine firing time = 57 sec
1 st	0.258	0.224	0.773	0.516
2 nd	.254	.261	.781	.759
3 rd	.250	.270	.804	.790

E-6881

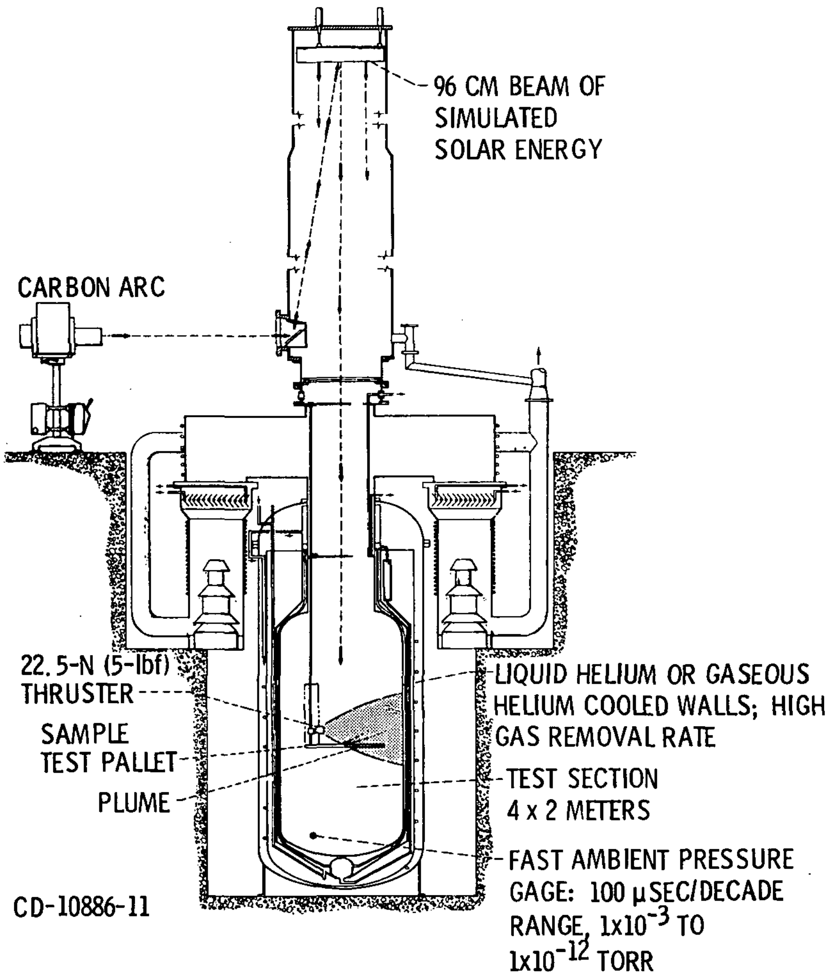

Figure 1. - Liquid helium cooled space simulator and thruster installation.

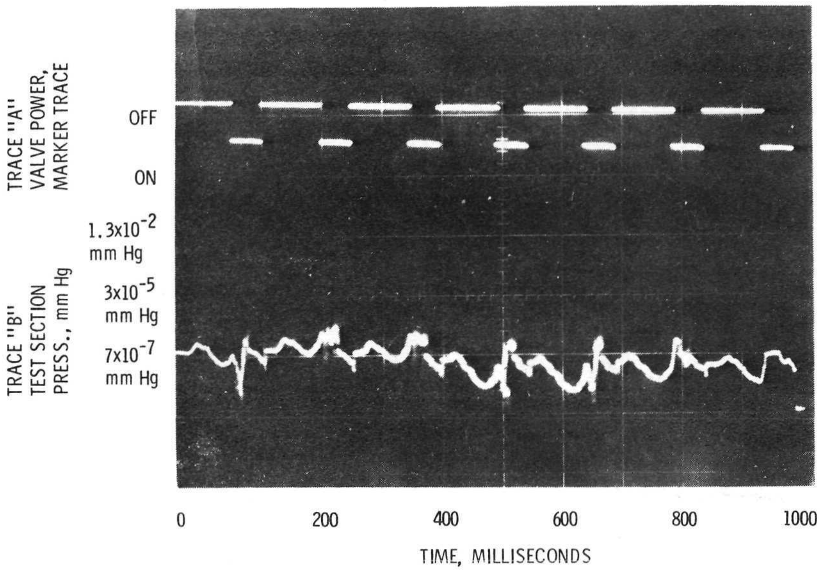

Figure 2. - Space chamber pressure during rocket firing.

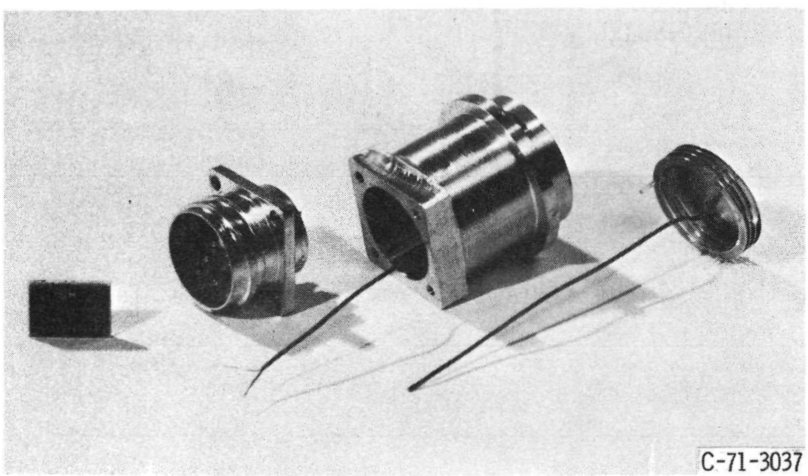

Figure 3. - Sample and mounting cup assembly.

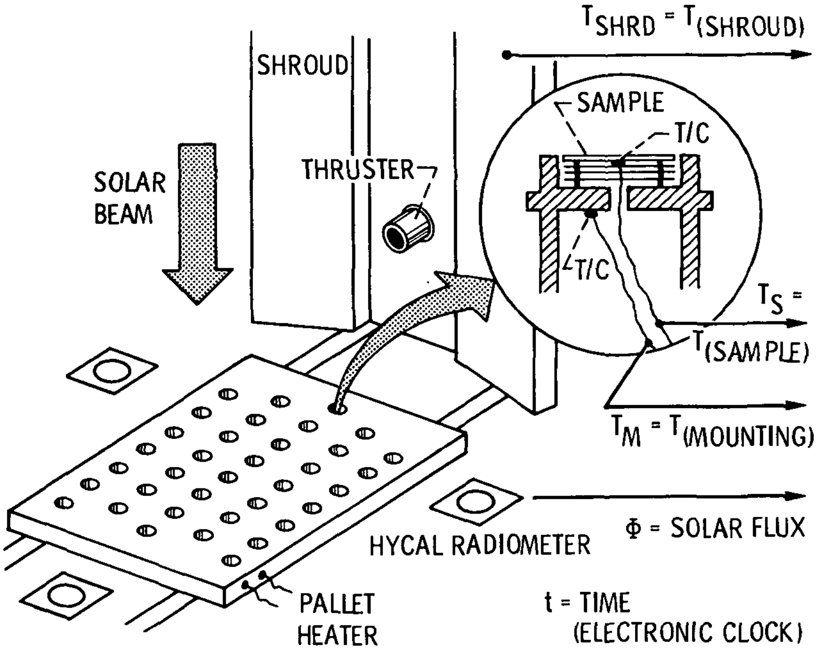

Figure 4. - Sample arrangement.

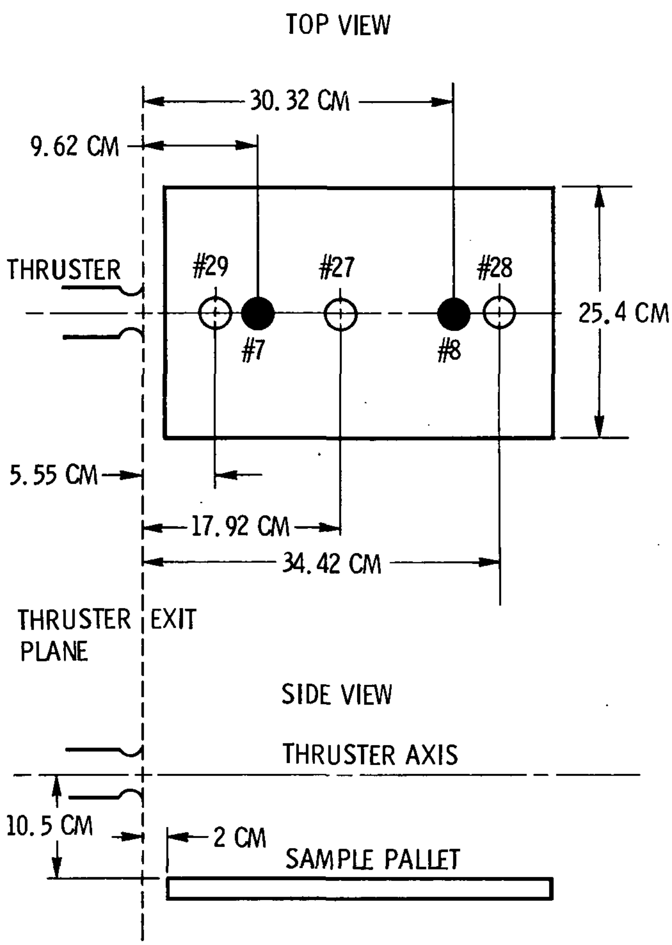

Figure 5. - Sample locations.

E-6881

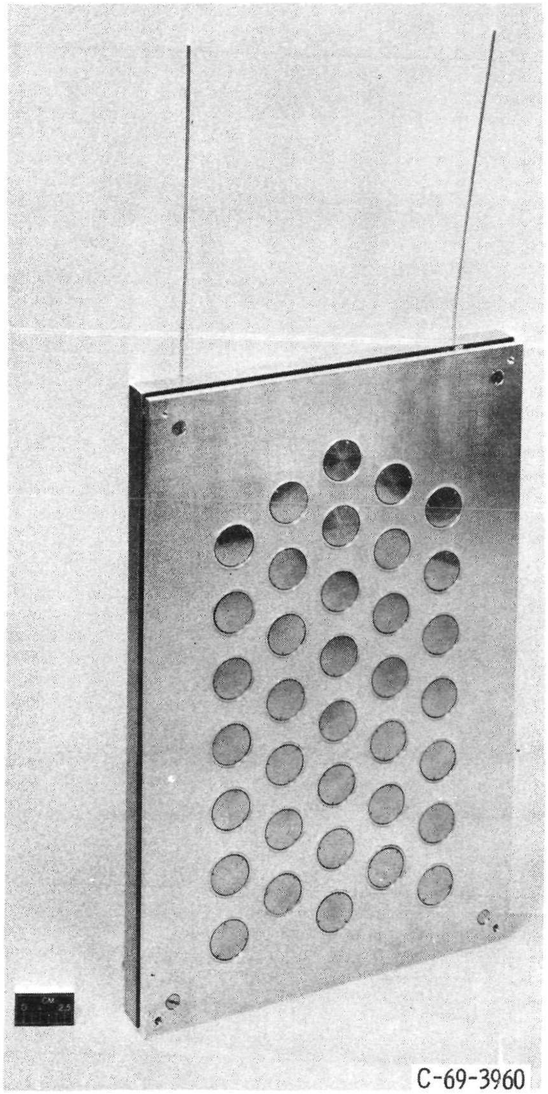

Figure 6. - Pallet with unpainted samples.

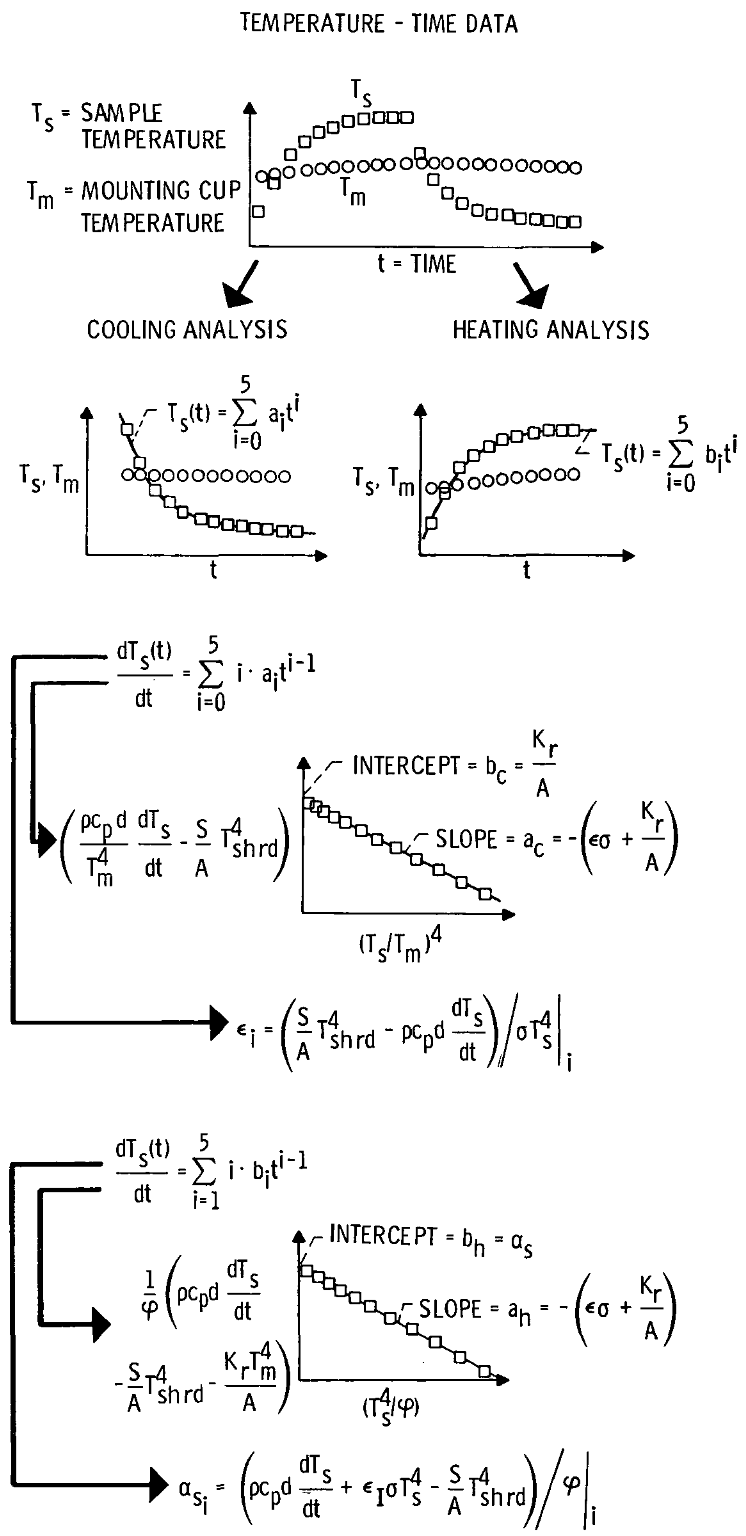

Figure 7. - Data analysis - schematic organization.

E-6881

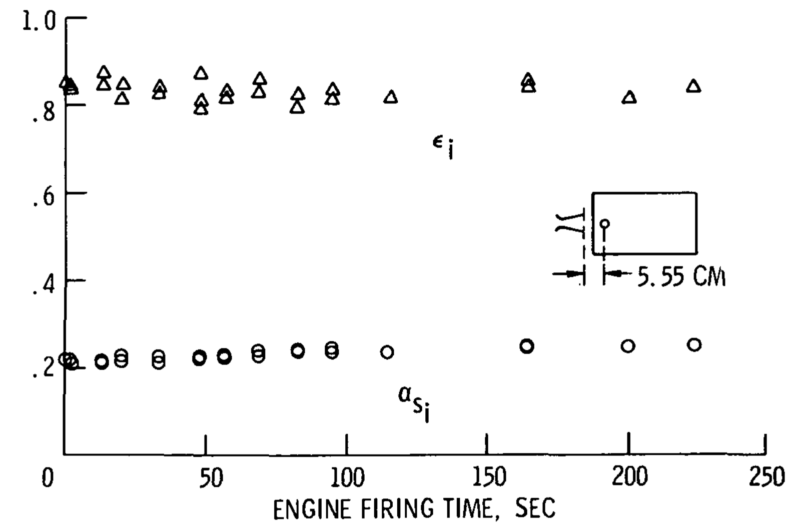

(a) S13G, SAMPLE NO. 29.

Figure 8. - Emittance (ϵ_i) and solar absorptance (α_{s_i}) of S13G coating.

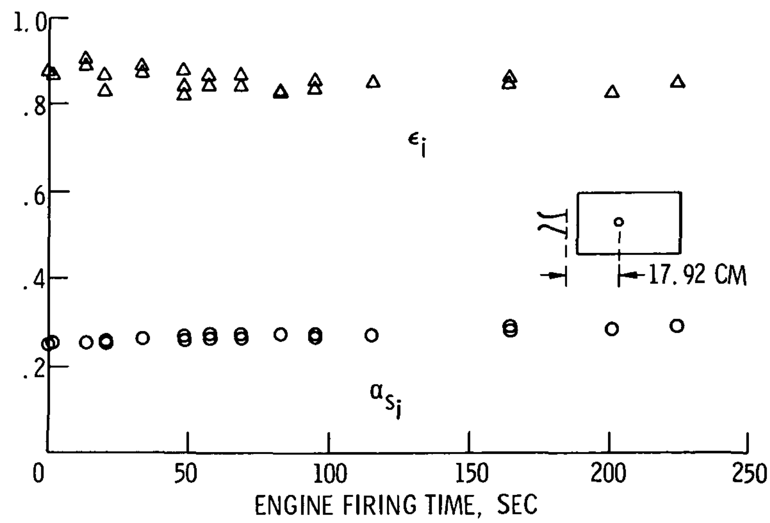

(b) S13G, SAMPLE NO. 27.

Figure 8. - Continued.

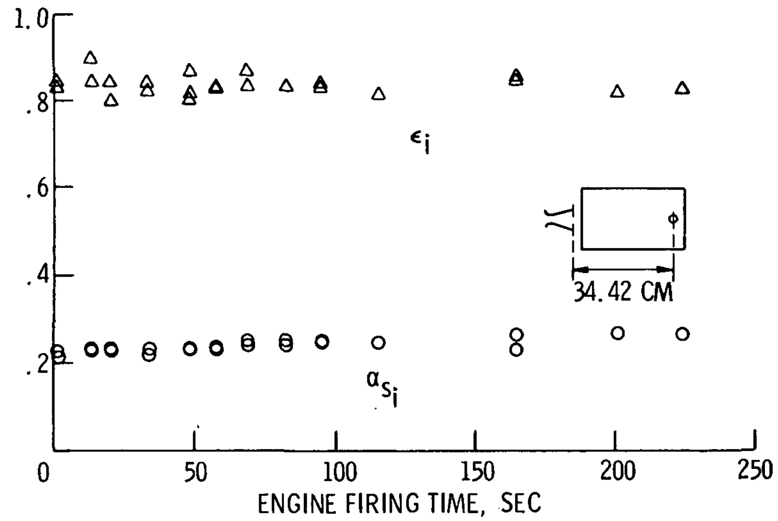

(c) S13G, SAMPLE NO. 28.

Figure 8. - Concluded.

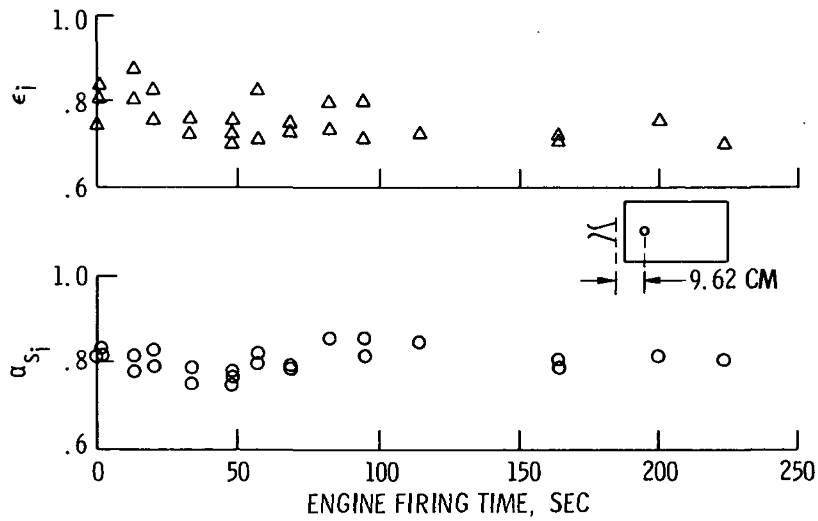

(a) CAT-A-LAC BLACK, SAMPLE NO. 7

Figure 9. - Emittance (ϵ_i) and solar absorptance (α_{s_i}) of Cat-a-lac black coating.

E-6881

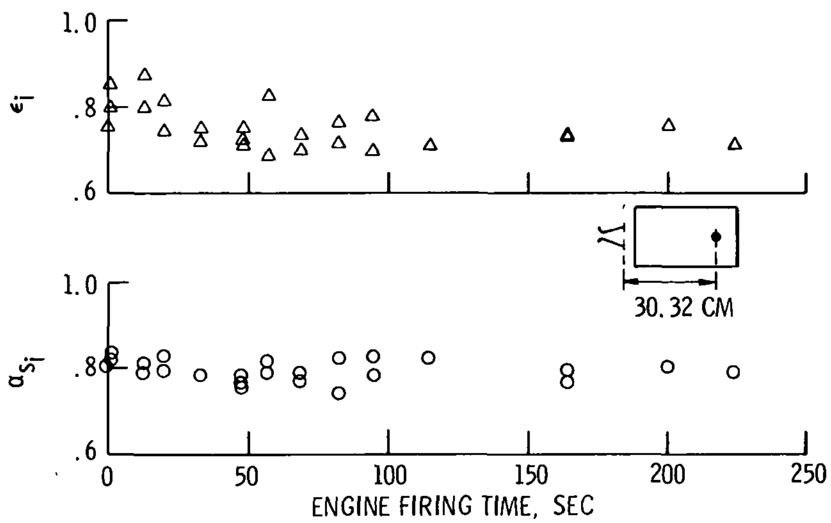

(b) CAT-A-LAC BLACK, SAMPLE NO. 8.

Figure 9. - Concluded.